



ELSEVIER

Physica B 221 (1996) 261–266

PHYSICA B

Surface freezing and surface-phase behaviors in binary mixtures of alkanes

X.Z. Wu^{a,b,c,*}, B.M. Ocko^d, M. Deutsch^e, E.B. Sirota^c, S.K. Sinha^{b,c}^a *Physics Department, Northern Illinois University, DeKalb, IL 60115, USA*^b *Argonne National Laboratory, Argonne, IL 60439, USA*^c *Exxon Research and Engineering Co., Route 22 East, Annandale, NJ 08801, USA*^d *Physics Department, Brookhaven National Laboratory, Upton, NY 11973, USA*^e *Physics Department, Bar Ilan University, Ramat Gan 52900, Israel*

Abstract

X-ray surface scattering and surface tension measurements reveal surface freezing in molten mixtures of alkanes of two different lengths. A crystalline monolayer is formed at the surface a few degrees *above* the bulk freezing temperature. The structure of the monolayer has been determined on an angstrom scale. Two widely different patterns of behavior emerge, which depend on the length difference of the two components, Δn . For small Δn the surface properties and structure vary continuously with concentration. For large Δn , however, the variation is discontinuous, exhibiting surface segregation. Furthermore, a new surface crystalline structure appears for a well-defined range of compositions and temperatures, and surface freezing is completely suppressed for another range. A Flory–Huggins theory based on competition between entropic mixing and a repulsive interaction due to chain length mismatch accounts well for the observed phenomena.

1. Introduction

Molecules residing at a free surface of a solid are less confined than those in the bulk [1–4]. The consequently larger entropy at the surface results in a lower melting temperature at the surface than in the bulk. This so-called surface melting phenomenon is a general prediction of statistical physics and has been observed in numerous systems ranging from ice [5], through metals [4] to molecular crystals [6]. The opposite phenomenon, that of surface freezing, where the surface solidifies at a temperature *higher* than that of the bulk is much more rare. In fact, prior to the discovery of surface freezing in alkanes, it had only been observed in liquid crystals [7].

Very recently we [8–10], and others [11,12], found that pure monodisperse liquid normal alkanes ($\text{CH}_3(\text{CH}_2)_{n-2}\text{CH}_3$, abbreviated as C_n) also exhibit surface freezing. Here a crystalline monolayer is formed on the surface of the melt at temperatures of up to a few degrees above the bulk freezing point. While this is clearly a result of a delicate balance between the bulk and surface free energies, the microscopic details of the physics underlying this effect are still unclear. To gain a better understanding, we have studied the surface behavior of liquid binary mixtures of n-alkanes, where the bulk free energies can be tuned conveniently by varying the molecular lengths and the compositions. As we show below, the new dimensions in phase space accessible to mixtures not only help in understanding the basic phenomenon, but may also induce new phenomena which do not occur

* Corresponding author.

in the pure components. Furthermore, alkanes in “real world” applications generally exist in the form of mixtures [13]. Even “pure” alkanes are seldom monodisperse, and are usually laced with varying amounts of similar shorter- and longer-chain molecules. Thus, the study of alkane mixtures presented here is relevant not only to basic science but also to applied science and industrial applications.

As the surface freezing in alkane mixtures is closely related to that in monodisperse alkanes, we now summarize the results obtained for pure alkanes. The crystalline monolayer is formed at a temperature $T_s > T_f$, where T_f denotes the bulk freezing temperature. The liquid–solid surface transition is first order. Once formed, the structure of the monolayer remains invariant upon further cooling down to bulk freezing at T_f . The temperature range of existence, $\Delta T = T_s - T_f$, of this surface crystalline phase has a non-monotonic molecular length dependence. It tends to go to zero for $n < 16$ and $n > 52$, and has a maximum of about 3 °C for $n \sim 20$. The monolayer has a structure similar to that of the bulk R_{II} rotator phase [21], where there is long-range average positional and orientational order, but no long-range order of molecular rotation along their long axes. The surface crystalline coherence length is at least a few thousand Å. For chain lengths $n < 30$ the chains are stretched and oriented normal to the surface, and packed hexagonally. For $n \geq 30$ the molecules are tilted towards their nearest neighbours, with the tilt angles increasing with n and reaching 18° for C_{36} . Further details are given in Refs. [8–10].

In the study reported here, we show that surface freezing occurs in binary mixtures of alkanes as well. As in pure alkanes the surface freezing occurs via a reversible first-order transition. The surface layer is always crystalline and a single monolayer thick. However, since the interactions among alkane molecules and their affinity to the surface differ with chain length, both the temperature range of the surface crystalline phase and the surface composition vary with the length difference Δn and bulk composition. By varying the concentration in the bulk liquid it is now possible to fine-tune the free energy balance and obtain for a particular range a complete exclusion of one of the components from the surface or even a complete suppression of the surface freezing effect. For mixtures with small Δn , the crystalline surface layer is a uniform mixtures of the two components. For large Δn , only one component of the bulk binary mixture appears in the surface crystalline layer. We have studied extensively two families of alkane mixtures, $C_{20} - C_{20 + \Delta n}$ and $C_{36 - \Delta n} - C_{36}$, where Δn ranges from 2 to 18. The Δn dependence of the surface phase behavior is found to be very similar for both families. These results are discussed below in detail.

2. Experimental

Each sample was prepared by thoroughly stirring a preweighed, molten mixture of commercial alkanes of purity $\geq 99\%$. The molten mixture was then poured onto a clean silicon wafer mounted in a sealable cell, the temperature of which was regulated to within 5 mK. The surface structure of the liquid mixture was studied by X-ray reflectivity (XR) and X-ray grazing incidence diffraction (GID), using the Harvard/BNL liquid spectrometer at beamline $\times 22B$ of the National Synchrotron Light Source. The surface thermodynamic properties were measured using the surface tension (ST) technique. XR yields information on the electron density profile normal to the surface [14], such as the thickness and density of a surface film. GID measurements provide information on the structure of a film within the surface plane [15]. The orientation of the molecular chains is obtained from the Bragg-rods (BR), i.e. the surface-normal dependence of the scattered intensity at the position of each in-plane GID peak. The ST measurements, using the Wilhelmy plate method [10, 16], provide information on the excess free energy of the molecules at the surface over those in the bulk. The formation of the layer at T_s is seen as a sharp change from a negative to a positive slope in the surface tension $\gamma(T)$ and the slope difference $\Delta(d\gamma/dT)$ increases linearly with the carbon number n [10].

3. Results and discussion

Fig. 1 shows XR measured for the free surfaces of monodisperse C_{32} and C_{36} alkanes and their equal volume mixture. At $T > T_s$, no surface layer is present, and a monotonic fall-off with q_z , typical of an isotropic liquid surface [17], is observed for all samples. At temperatures below T_s , but still above the bulk freezing temperature T_f ($T_f \leq T \leq T_s$), the XR curves for all three samples exhibit pronounced modulations, indicating the existence of a surface layer with an electron density different from that of the bulk. The different modulation periods reflect different average surface layer thicknesses D . The XR data were fitted using a model assuming a layered interface consisting of a slab of higher electron density (representing the ordered $(CH_2)_{n-2}$ chains), and a lower-density depletion zone at the layer-liquid interface (corresponding to the less dense CH_3 groups). This is the same model used to fit the crystalline monolayers of the monodisperse n -alkanes [8]. The fit yields the density profiles shown in the inset. A 15% increase in the density of the surface layer over that of the liquid bulk is found for all mixtures. Note that D for the small Δn mixtures ($C_{32} - C_{36}$ in Fig. 1) is intermediate between those for the

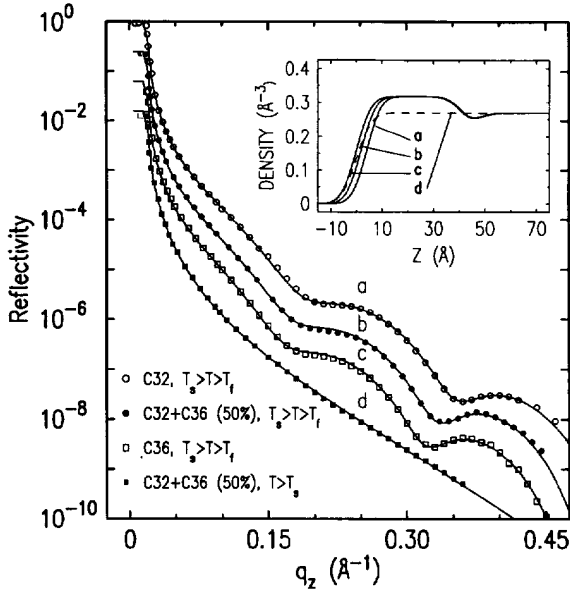


Fig. 1. X-ray reflectivities from the free surface of molten n-alkanes C_{32} and C_{36} in their surface crystalline phase, and their 1:1 mixtures in both the surface crystalline and the higher-temperature liquid phase. The solid lines are fits according to density profiles shown in the inset. The reflectivities are shifted for clarity by a factor of 4 each.

two pure materials. This indicates that the mixture behaves similar to a monodisperse alkane of an intermediate chain length in this case. A similar behavior was observed in binary mixtures of close homologues in several liquid crystal families [18].

Figs. 2(a) and (b) displays the surface crystalline layer thickness as a function of compositions for two typical mixtures: $C_{30} + C_{36}$ representing the small Δn mixtures, and $C_{26} + C_{36}$ representing the large Δn ones. For the first of these, the average D varies continuously and monotonically with ϕ_{30} (the volume fraction of C_{30} in the bulk liquid), between those of pure C_{30} and C_{36} . This continuous variation of D implies a continuous change in the composition of the surface crystalline layer, $D = \phi^{cs}D_{30} + (1 - \phi^{cs})D_{36}$, here ϕ^{cs} is the C_{30} concentration in the surface crystalline layer and D_{30} and D_{36} are the layer thickness of pure C_{30} and C_{36} , respectively. The solid curves represent the values of D estimated from the theory discussed below, which is based on the value derived for ϕ^{cs} . Since the entropy depends linearly on the chain length [10], a linear relation is also expected in the ST measurements between the thickness D and the surface tension slope $\Delta(d\gamma/dT) \approx \Delta S$. This is indeed observed, as shown in the inset of Fig. 2(a).

The large Δn C_{26} – C_{36} mixtures exhibit, by contrast, a dramatically different surface behavior, as shown in

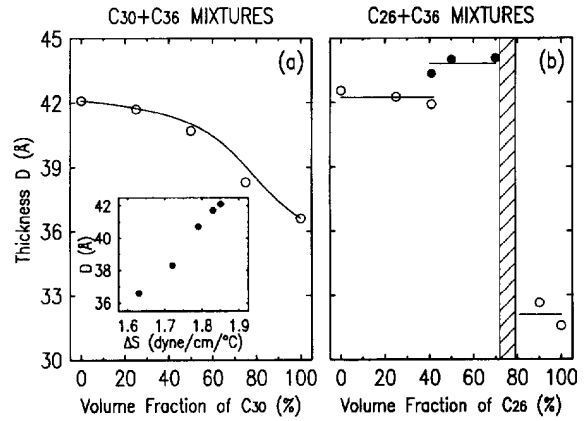


Fig. 2. (a) For the C_{30} – C_{36} mixture series, the thickness of the crystalline surface layer is plotted as a function of ϕ_{30} . The solid lines are the theoretical values based on the calculated surface crystalline composition as discussed in the text. The inset shows the thickness as a function of the entropy difference between the liquid and crystalline surface phases as derived from the measured surface tension slope differences $\Delta S = \Delta(d\gamma/dT)$. (b) The corresponding plots for the C_{26} – C_{36} mixtures. The solid circles denote the new surface phase. Surface freezing is absent in the shaded regions.

Fig. 2(b). The thickness D varies discontinuously with ϕ_{26}^l . It takes on three discrete values, shown in solid lines in Fig. 2(b). For $\phi_{26}^l > 80\%$, and $\phi_{26}^l < 40\%$, D are those of pure C_{26} and C_{36} , respectively. In both cases the surface crystalline layer appears to consist of a single component: either C_{26} or C_{36} . For a range of ϕ_{26}^l between 70% and 80% (the shaded region in Fig. 2(b)) the surface freezing effect disappears completely. Finally, for $40\% < \phi_{26}^l < 70\%$, a new surface phase appears via a first-order transition [19]. In this region D is even slightly larger than that of pure C_{36} . A similar division into four regions, with identical temperature boundaries is observed in the surface tension measurements.

The GID measurements reveal that the in-plane ordering of the crystalline surface layers of the mixtures, other than in the new phase, is the same as that in the corresponding monodisperse phase. For example, for the ordinary, $\phi_{26}^l < 40\%$ surface crystalline phase in the C_{26} – C_{36} mixture, where the C_{36} segregates to the surface, there exists only one resolution-limited GID peak at $q = 1.48 \text{ \AA}^{-1}$, as shown in Fig. 3(a). Bragg rod measurements at the position of this peak show two maxima, one at $q_z = 0$ and another at $q_z = 0.5 \text{ \AA}^{-1}$ (Fig. 3(b)). As shown in Ref. [9] these are consistent with a hexagonal packing of molecules tilted towards their nearest-neighbors by 18° , exactly as found for pure monodisperse C_{36} . For the new surface phase, shown in Figs. 3(c) and (d) the position q of the in-plane peak remains the same

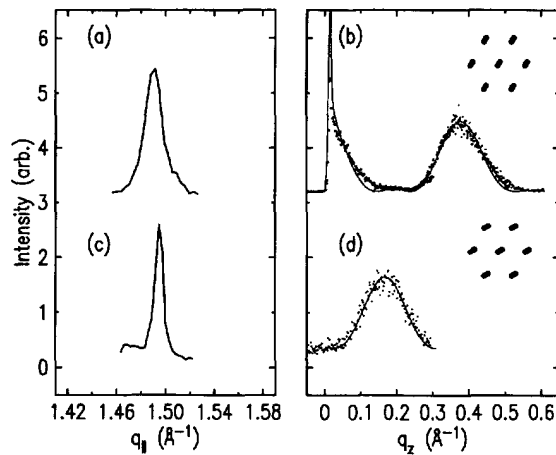


Fig. 3. The in-plane diffraction peaks for the crystalline surface phase of C_{26} – C_{36} mixtures in (a) the ordinary surface crystalline phase ($\phi_{26}^l < 40\%$), and (b) the new phase ($40\% < \phi_{26}^l < 60\%$). Both peaks are resolution limited, indicating crystalline coherence length in excess of a few thousand Å. The corresponding vertical, q_z , distribution of the intensity at the in-plane diffraction peak position, the so-called Bragg rods, are shown in (c) and (d) for the two phases, respectively. For their discussion see text.

(Fig. 3(c)). However, the $q_z = 0$ peak disappears and only one peak at $q_z > 0$ is detected (Fig. 3(d)). This is consistent with a tilt towards next-nearest-neighbors. The lower q_z position of the Bragg rod peak as compared to Fig. 3(b) indicates that the tilt angle is now decreased to 13.5° . This, in turn, should increase the layer thickness D , as was indeed observed in the values of D derived from the reflectivity measurements (see Fig. 2(b)). Note, however, that such a packing entails a second peak, of a much lower intensity, along the Bragg rod at a higher q_z . This was not observed in the measurements. While this may be due to the low intensity expected, in the absence of this peak other structural models cannot be ruled out completely.

The measured quantities such as the monolayer thickness D and slope difference $\Delta(d\gamma/dT)$ are temperature independent for $T_f < T < T_s$ for a fixed concentration ϕ_{26}^l . However, for a concentration range of a few percent around $\phi_{26}^l \approx 40\%$, where the transition to the new phase occurs, it is possible to tune the system between the usual phase and the new surface phase by varying the temperature. The transition to the new phase is invariably found to occur at $T_{\text{new}} \approx 69^\circ\text{C}$, for all bulk compositions. Moreover, the transition from the usual to the new phase was also observed in other $C_{36} + C_{36-\Delta n}$ mixtures with $\Delta n \geq 10$, with the transition always occurring at the same $T_{\text{new}} \approx 69^\circ\text{C}$, independent of Δn and concentration within the allowed range. Therefore, it is proposed that

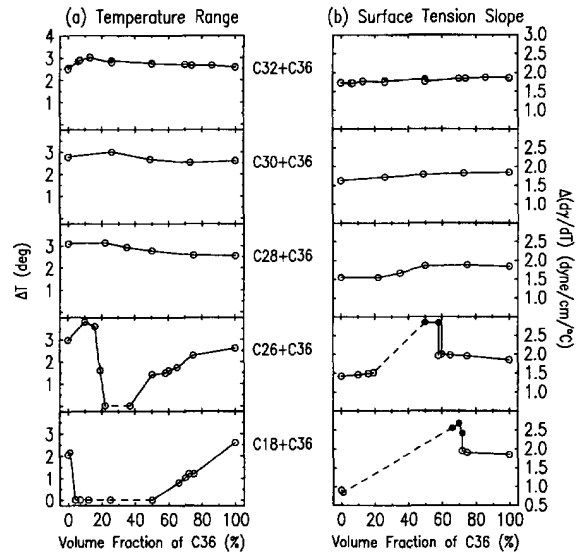


Fig. 4. For $C_{36} + C_{36-\Delta n}$ mixtures, with Δn varying between 4 and 18: (a) The temperature range of existence of the crystalline surface layer, ΔT , as a function of the liquid bulk composition. (b) The slope difference of the surface tension, $\Delta(d\gamma/dT)$, as a function of liquid bulk composition. The lines connecting the points for each mixture are guides to the eye, and the dashed line marks the region where surface freezing does not occur. The solid symbols denote the new surface phase discussed in the text.

$T_{\text{new}} = 69^\circ\text{C}$ is the transition temperature intrinsic to the C_{36} surface crystalline layer, independent of the underlying liquids, whereas the surface and bulk freezing temperatures T_s and T_f are determined by the bulk liquid compositions. This new surface phase will occur only when $T_{\text{new}} > T_f$, and be inducible by temperature variation only when $T_s > T_{\text{new}} > T_f$ [19]. Since T_s and T_f are dependent on, while T_{new} is independent of the bulk composition, the volume fractions at which the transition between the new and normal surface phases occurs is different for different families of mixtures.

The temperature range of existence of the surface crystalline phase, ΔT , is shown in Fig. 4(a) versus the bulk composition for different mixtures. A dramatically different behavior is observed for small and large Δn . For $\Delta n < 9$, ΔT is practically constant, with a slight enhancement in the $20\% < \phi < 40\%$ range. For $\Delta n > 9$, however, ΔT changes abruptly with bulk composition, and there exists a region where surface freezing is suppressed completely (i.e. $\Delta T = 0$). This region increases with increasing Δn . This behavior results from the fact that the ϕ dependence of the two transition temperatures T_s and T_f are very different for these Δn .

The difference in the slope, $\Delta(d\gamma/dT)$, of the surface tension $\gamma(T)$ below and above T_s is the entropy loss ΔS

of the surface layer in the transition from liquid to crystalline [10]. In monodisperse alkanes, $\Delta(d\gamma/dT)$ increases linearly with the carbon numbers. In mixtures, they are displayed in Fig. 4(b) as a function of the bulk composition for samples of various Δn . For mixtures of $\Delta n < 9$, $\Delta(d\gamma/dT)$ changes continuously between the values of the two pure components. Continuous intermediate values of $\Delta(d\gamma/dT)$ imply continuous changes in the composition of the surface crystalline layer. For mixtures of $\Delta n > 9$, $\Delta(d\gamma/dT)$ takes on the discrete values of the pure components, indicating that predominantly only one component is present in the surface crystalline phase. These single component surface phase regions are separated from one another by a region where the surface freezing is suppressed. This could result from frustration due to the competition between closely matched surface segregation affinities of the two species. In a narrow region just outside this no-freezing region, $\Delta(d\gamma/dT)$ takes on values which are even larger than the largest of the two pure components' values, as marked by the solid symbols in Fig. 4(b). This is the region of existence of the new surface phase discussed above in the context of the X-ray measurements. The surface tension slope change $\Delta(d\gamma/dT)$ at this transition is consistent with entropy change ΔS from a rotator to crystal phase transition, which occurs at $\sim 73^\circ\text{C}$ in bulk C_{36} [21]. We, therefore, speculate that the rotational degree of freedom is frozen out at this transition.

The phase behavior described above, and, in particular, the pronounced Δn dependence, can be accounted for extremely well by a Flory–Huggins-type theory of the binary mixture [19]. This theory describes the system energetics by basically two competing interactions: the entropic mixing and the repulsive interaction due to chain length mismatch [22]. The first of these drives for a uniform mixing of the two components. The second tries to minimize the contact between ordered chains of different lengths, i.e. drives for phase separation of the two components. The equilibrium state is determined by the balance of the two. The repulsive interaction due to chain length mismatch was taken to be proportional to $(\Delta n/\bar{n})^2$, where \bar{n} is the average chain length. Other ingredients determining the phase boundaries are the properties of the pure components and the composition of the bulk liquid mixture. The model then uses these to obtain the coefficient of the repulsive interaction, the surface freezing temperature and the composition of the crystalline surface and bulk phase at freezing. This simple thermodynamic model was found to describe quantitatively the overall phase behavior, including the transition temperatures and the surface and bulk compositions. The prediction for D is given as a solid line in Fig. 2(a) and can be seen to be in good agreement with the measurements. The theory accounts, in particular, for the fact that for

$\Delta n/\bar{n} \approx 9/32 \approx 0.3$ the surface crystalline layer changes from a mixed, continuous behavior to a segregated, discontinuous one. Further details will be published elsewhere [19,20].

This is the first molecular-resolution study of the phase diagram of the free surface of a liquid binary mixture, to the best of our knowledge. It reveals several rare or unique phenomena in these systems such as surface freezing, a new surface phase and a surface phase transition between two distinct crystalline structures. Δn was found to tune the system between two dramatically different behavioral patterns. Further studies, over a larger range of chain lengths and on different materials are in progress to elucidate the surface phase behavior in chain molecules and its relations with the phase behavior of the bulk.

Acknowledgements

This work was supported in part by the US–Israel Binational Science Foundation, Jerusalem and Exxon Education Foundation. BNL is supported by the Division of Materials Research, DOE under contract DE-AC02-76CH00016.

References

- [1] J.G. Dash, *Contemp. Phys.* 30 (1989) 89.
- [2] R. Lipowsky, *J. Appl. Phys.* 55 (1984) 2485 and references therein.
- [3] G. An and M. Schick, *Phys. Rev. B* 37 (1988) 7534.
- [4] J.W.M. Frenken and J.F. van der Veen, *Phys. Rev. Lett.* 54 (1985) 134; H. Dosch, T. Höfer, J. Peisl and R.L. Johnson, *Europhys. Lett.* 15 (1991) 527.
- [5] M. Elbaum and M. Schick, *Phys. Rev. Lett.* 66 (1991) 1713.
- [6] S. Chandavarkar, R.M. Geertman and W.H. de Jeu, *Phys. Rev. Lett.* 69 (1992) 2384.
- [7] P.S. Pershan and J. Als-Nielsen, *Phys. Rev. Lett.* 52 (1984) 759; D.E. Moncton, R. Pindak and S.C. Davey, *Phys. Rev. Lett.* 49 (1982) 1865; B.M. Ocko, A. Braslau, P.S. Pershan, J. Als-Nielsen and M. Deutsch, *Phys. Rev. Lett.* 57 (1986) 94; E.B. Sirota, P.S. Pershan, S. Amador and L.B. Sorensen, *Phys. Rev. A* 35 (1987) 2283; G.J. Kellogg, P.S. Pershan, E.H. Kawamoto, W.F. Foster, M. Deutsch and B.M. Ocko, *Phys. Rev. E* 51 (1995) 4709.
- [8] X.Z. Wu, E.B. Sirota, S.K. Sinha, B.M. Ocko and M. Deutsch, *Phys. Rev. Lett.* 70 (1993) 958.
- [9] X.Z. Wu, M. Deutsch, B.M. Ocko, E.B. Sirota and S.K. Sinha, to be published.
- [10] X.Z. Wu, B.M. Ocko, E.B. Sirota, S.K. Sinha, M. Deutsch, B.H. Cao and M.W. Kim, *Science* 261 (1993) 1018.
- [11] J.C. Earnshaw and C.J. Hughes, *Phys. Rev. A* 46 (1992) R4494.
- [12] G.A. Seffler, Q. Du, P.B. Miranda and Y.R. Shen, *Chem. Phys. Lett.* 235 (1995) 347.

- [13] E.B. Sirota, H.E. King Jr., H.H. Shao and D.M. Singer, *J. Phys. Chem.* 99 (1995) 798 and references therein.
- [14] J. Als-Nielsen, F. Christensen and P.S. Pershan, *Phys. Rev. Lett.* 48 (1982) 1107; T.P. Russell, *Mat. Sci. Rep.* 5 (1990) 171.
- [15] J. Als-Nielsen and K. Kjær, in: *Phase Transitions in Soft Condensed Matter*, eds. T. Riste and D. Sherrington (Plenum, New York, 1989); D.K. Schwartz, M.L. Schlossman and P.S. Pershan, *J. Chem. Phys.* 96 (1991) 2356.
- [16] G.L. Gaines, *Insoluble Monolayers at the Liquid Gas Interface* (Wiley, New York, 1966).
- [17] A. Braslau, P.S. Pershan, G. Swislow, B.M. Ocko and J. Als-Nielsen, *Phys. Rev. A* 38 (1988) 2457; M.K. Sanyal, S.K. Sinha, K.G. Huang and B.M. Ocko, *Phys. Rev. Lett.* 66 (1991) 628; B.M. Ocko, X.Z. Wu, E.B. Sirota, S.K. Sinha and M. Deutsch, *Phys. Rev. Lett.* 72 (1994) 242.
- [18] B.M. Ocko R.J. Birgeneau and J.D. Litster, *Z. Phys. B: Condens. Matter* 62 (1986) 487; L. Chen, J.D. Brock, J. Huang and S. Kumar, *Phys. Rev. Lett.* 67 (1991) 2037.
- [19] X.Z. Wu, B.M. Ocko, H. Tang, E.B. Sirota, S.K. Sinha and M. Deutsch, *Phys. Rev. Lett.* 75 (1995) 1332.
- [20] X.Z. Wu, B.M. Ocko, H. Tang, A. Doerr, O. Gang, M. Deutsch, E.B. Sirota, S.K. Sinha and M. Deutsch, to be published.
- [21] D.M. Small, *The Physical Chemistry of Lipids* (Plenum, New York, 1986).
- [22] L.E. Reichl, *A Modern Course in Statistical Physics* (University of Texas, Texas, 1980); P. Flory, *Principles of Polymer Chemistry* (Cornell, Ithaca, 1953).